

# Aggregate Human Mobility Modeling Using Principal Component Analysis\*

Jingbo SUN

*Department of Electronic  
Engineering, Tsinghua  
University, Beijing, China  
sjb06@mails.tsinghua.edu.cn*

Yue WANG

*Department of Electronic  
Engineering, Tsinghua  
University, Beijing, China  
wangyue@tsinghua.edu.cn*

Hongbo SI

*Department of Electronic  
Engineering, Tsinghua  
University, Beijing, China  
sihb07@mails.tsinghua.edu.cn*

Jian YUAN

*Department of Electronic Engineering  
Tsinghua University, Beijing, China  
jyuan@tsinghua.edu.cn*

Xiuming SHAN

*Department of Electronic Engineering  
Tsinghua University, Beijing, China  
shanxm@tsinghua.edu.cn*

## Abstract

Accurate modeling of aggregate human mobility benefits many aspects of cellular mobile networks. Compared with traditional approaches, the cellular networks provide information for aggregate human mobility in urban space with large spatial extent and continuous temporal coverage, due to the high penetration of cell phones. In this paper, a model by utilizing Principal Component Analysis (PCA) is proposed to explore the space-time structure of aggregate human mobility. The original data were collected by cellular networks in a southern city of China, recording population distribution by dividing the city into thousands of pixels. By applying PCA to original data, the low intrinsic dimensionality is revealed. The structure of all the pixel population variations could be well captured by a small set of eigen pixel population variations, an introduced notion capturing significant temporal patterns across all the pixel population variations. According to their temporal features, eigen pixel population variations can be divided into three categories, and each pixel population variation can be decomposed into three corresponding constitutions: deterministic trends, short-lived spikes, and noise. Furthermore, there is also a relation between the variance of a pixel population variation and its dominated constitution. The most significant eigen pixel population variations are utilized in the applications of forecasting and anomaly detection.

## 1 Introduction

Accurate modeling of human mobility is of great benefit in many aspects of cellular mobile networks, including network planning, location management and resource management [2]. The studies about human mobility are usually divided into two classifications: individual and aggregate. The former discusses the movement trajectory of only one person [6], while the latter investigates the overall movement behavior of large crowds. This paper focuses on aggregate human mobility, which can be also called “urban dynamics” in urban environment. It may facilitate the provision of public services to all citizens, such as public safety, public transportation, and other group-directed services.

The researches of aggregate human mobility also have two categories. One category is synthetic model, such as gravity model [9] and fluid flow model [16], which is not precise enough. The other category belongs to measurement-based model. The traditional approaches of collecting data are just snapshots and provide no temporal coverage, e.g. surveys and gate counts. With the help of mobile devices capable of collecting data immediately, some groups of trace data are acquired involving several hundreds of participants at most [1, 4, 10], but the spatial extent is very limited. In comparison with the

---

*Journal of Wireless Mobile Networks, Ubiquitous Computing, and Dependable Applications*, volume: 1, number: 2/3, pp. 83-95

\*An abbreviated version of this paper appeared in [15].

existing methods, the cellular networks provide information for urban dynamics with large spatial extent and continuous temporal coverage, due to the high penetration of cell phones. However, the utilization of the data generated daily by the cellular mobile networks is relatively rare, as the result of the obstacle of data access from telecommunications carriers.

The ‘‘Real Time Rome’’ project [3], under the cooperation between MIT and Telecom Italy in 2006 is the first work of this area [14]. It regards Erlang data, which is a measure of network bandwidth consumption, as an indicator to human behaviors in urban activities. Based on Erlang data, cluster analysis of all the ‘‘pixels’’ is done in Rome [14], while a similar study is carried out in Milan [12]. The spatiotemporal behaviors in Rome were investigated by extracts recurring patterns of mobile phone usage on a separate single place [13]. However, the works mention above explore the temporal and spatial patterns of urban dynamics separately, i.e. either temporal patterns on one place or space patterns at one moment.

In this paper, we explore the spatial and temporal structure of urban dynamics as a whole. The original data were collected in a southern city of China, and presented by dividing the city into thousands of pixels. Due to the high dimension of the pixels, Principal Component Analysis (PCA) [7] is employed to explore lower-dimensional representation termed an intrinsic dimensionality. We refer to the difference of population in one pixel between two sampling moments as Pixel Population Variation (PPV). As the outcome of this PCA-based analysis, the notion of eigen pixel population variation (eigenPPV) is introduced and it is a time series capturing significant temporal patterns across all the PPVs.

This paper is organized as follows. The background knowledge about PCA and original data is introduced in Section 2. In Section 3, the results of analyzing PPVs by utilizing PCA are presented. Certain applications of this PCA-based approach are discussed in Section 4. Finally, Section 5 concludes the paper.

## 2 Background and Data

### 2.1 Principal Component Analysis

PCA is a simple, non-parametric method of dimension reduction for revealing the underlying structure in complex data. It re-expresses the original data with a new set of axes via coordinate transformation. The new axes, termed principal components, point to the directions with the largest remaining variance or energy in the data successively, under the assumption that the most important structure exists along the directions with the largest variance. Meanwhile, principal components are constrained to be mutually orthogonal. Because the energy that each principal component captures implies the relative importance along each direction, it appears that the structure of the complex original data might be well captured by the first few principal components. This is how the dimension reduction is done by applying PCA. This method has been applied in many areas, such as network traffic analysis [8].

Calculating principal components is intimately related to Singular Value Decomposition (SVD) [5]. We briefly introduce SVD in the rest of this subsection. Let  $\mathbf{X}$  be an  $n \times m$  matrix with rank  $r$ . It can be proved that its principal components are the eigenvectors of  $\mathbf{X}^T \mathbf{X}$ , a square, symmetric  $m \times m$  matrix:

$$\mathbf{X}^T \mathbf{X} \mathbf{v}_i = \lambda_i \mathbf{v}_i \quad i = 1, \dots, r \quad (1)$$

where  $\lambda_i$  is the non-zero eigenvalue corresponding to the  $m \times 1$  eigenvector  $\mathbf{v}_i$ .  $\mathbf{X}^T \mathbf{X}$  is a positive semidefinite matrix. Hence, the eigenvalues  $\{\lambda_i\}_{i=1}^r$  that capture the energy along each principal component are positive, and the eigenvectors  $\{\mathbf{v}_i\}_{i=1}^r$  are orthogonal with each other. By convention, the eigenvalues are usually ordered from large to small, and all the eigenvectors have unit length. Therefore  $\{\mathbf{v}_i\}_{i=1}^r$  are also the principal components of  $\mathbf{X}$ .  $\sigma_i \triangleq \sqrt{\lambda_i}$  ( $i = 1, \dots, r$ ) are the singular values.  $\mathbf{u}_i \triangleq \mathbf{X} \mathbf{v}_i / \sigma_i$  ( $i = 1, \dots, r$ )

are  $n \times 1$  vectors, which capture the structure of  $\mathbf{X}$ , termed as eigenPPV in the following sections. The larger the corresponding singular value  $\sigma_i$  is, the more significant  $\mathbf{u}_i$  is. It can be readily verified that  $\{\mathbf{u}_i\}_{i=1}^r$  are also orthogonal and of unit norm.

SVD can be also expressed in the form of matrix multiplication as:

$$\mathbf{X} = \mathbf{U}\Sigma\mathbf{V}^T \quad (2)$$

where  $\mathbf{U}$  has  $\{\mathbf{u}_i\}_{i=1}^r$  as its columns and  $\mathbf{V}$  has  $\{\mathbf{v}_i\}_{i=1}^r$  as its columns, in accordance with the order of singular values from large to small.  $\Sigma$  is an  $r \times r$  diagonal matrix with singular values on the diagonal. Thus, each column of  $\mathbf{X}$  can be written as:

$$\mathbf{X}_i = \sum_{j=1}^r v_{ij} \cdot (\sigma_j \mathbf{u}_j) \quad i = 1, \dots, m \quad (3)$$

where  $v_{ij}$  represents the entry of  $\mathbf{V}$  that lies in the  $i$ -th row and the  $j$ -th column. Equation (3) indicates that each column of  $\mathbf{X}$  is a linear combination of  $\{\mathbf{u}_i\}_{i=1}^r$  (scaled by its corresponding singular value). The truncated form of SVD is

$$\hat{\mathbf{X}} = \mathbf{U}_t \Sigma_t \mathbf{V}_t^T \quad (4)$$

where  $\hat{\mathbf{X}}$  is an approximation of  $\mathbf{X}$ . Only the first  $t$  columns of  $\mathbf{U}$ , the first  $t$  rows of  $\mathbf{V}^T$ , and the top-left part of  $\Sigma$  of size  $t$  are involved in calculation, with the rest entries of the matrices discarded. The variable  $t$  can be interpreted as the intrinsic dimensionality. Truncated SVD is actually a dimension reduction approach by PCA.

## 2.2 Original data

Original data of this research are collected by a system in the city of Shenzhen, supported by one telecommunications carrier in China. Shenzhen is one of Special Zones of China, covering an area of about two thousand square kilometers, and the whole population is more than fourteen million, with average density of more than seven thousand persons per square kilometer.

The system is called ‘‘Mobile Base Stations Based Dynamic Population Distribution Monitoring System’’ [17], which has started to operate from November of 2008. It can provide information about population distribution of the city continuously, in temporal scale of one hour and spatial scale of one kilometer. According to the design of system, the whole area is divided into 2268 pixels, shown in Figure 1. Every pixel is marked as its center point in the form of longitude and latitude pair, and its location error will not exceed 1 meter. In the temporal scale, the monitoring system updates its data within five minutes for each hour, including collecting, exchanging, gathering, calculating, storing and outputting the population data. Comparing with the local practical population information, the error of this monitoring system is limited in 5% for 90% of pixels and 10% for 99%.

## 3 Analysis of PPVs by PCA

In this section, we focus on the PPVs of downtown area lasting for a period of one week, since it is the most representative area of urban dynamic. This area consists of 105 pixels, numbered from 1 to 105, forming a  $15 \times 7$  rectangle. Hence, the measurement matrix is a  $167 \times 105$  matrix. Each column represents one single PPV, while each row denotes a snapshot of all the population variations of pixels at one moment. The results are presented below.

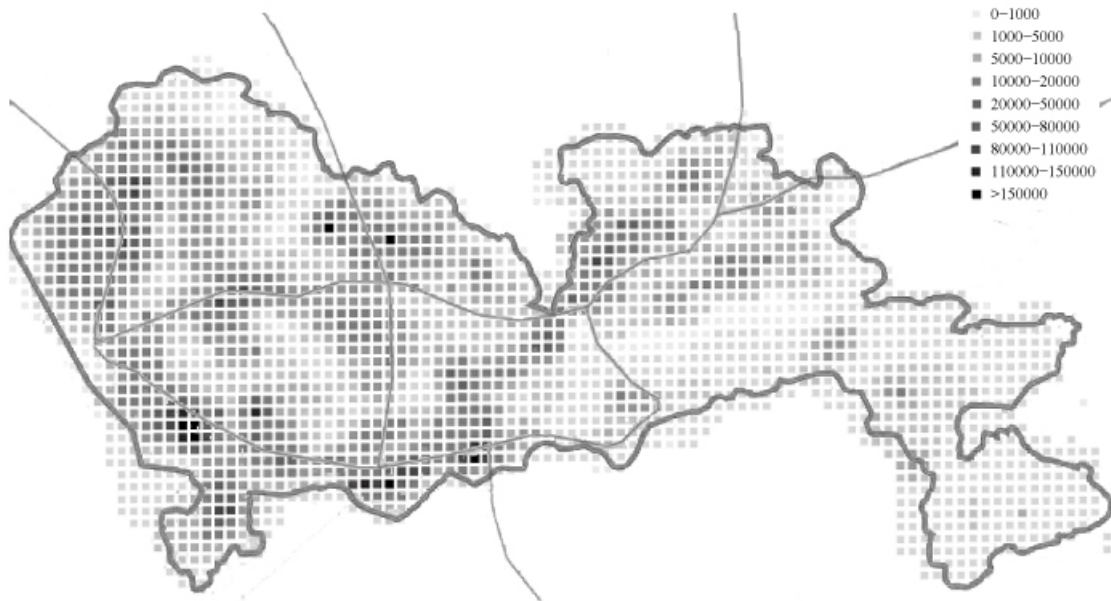


Figure 1: Population density distribution of Shenzhen.

### 3.1 Low intrinsic dimensionality of PPVs

Singular values and eigenPPVs can be calculated by applying PCA to the measurement matrix. Singular values, which represent the comparative significance of their corresponding eigenPPVs, are shown in Figure 2. There appears to be a very sharp elbow on the curve, which indicates the low intrinsic dimensionality of the structure. It seems that the first few eigenPPVs, around 10, could capture the structure of the ensemble of PPVs well. As shown in Figure 3, one randomly selected PPV can be accurately approximated by the most significant 10 eigenPPVs, even omitting most dimensions of PPVs.

### 3.2 Decomposition of PPVs

As stated by Equation (3), each PPV can be reconstructed as a weighted sum of eigenPPVs. However, each eigenPPV contributes to PPVs to different extents, which are specified by its corresponding principal component. An example of eigenPPV  $\mathbf{u}_3$  and its corresponding principal component  $\mathbf{v}_3$  is shown in Figure 4. It implies that eigenPPV  $\mathbf{u}_3$  contributes most to PPV 85.

Since principal components correspond to rows of  $\mathbf{V}$ , the extents to which eigenPPVs contribute are identified by their corresponding rows of  $\mathbf{V}$ . For the decomposition of one particular PPV, we only concern the eigenPPVs with relatively greater contribution, that is, the entries of the corresponding row of  $\mathbf{V}$ , whose absolute value is remarkably larger than zero. Hence, a reasonable threshold is required. If all the eigenPPVs contribute to one PPV equally, all the entries of the corresponding row of  $\mathbf{V}$  will be equal. Furthermore, each column of  $\mathbf{V}$  has unit norm, then one option of a reasonable threshold is  $1/\sqrt{m}$ .

For each row of  $\mathbf{V}$ , the number of entries which exceed  $1/\sqrt{m}$  in absolute value can be determined by setting this threshold. The notion of elements is introduced to represent the components with relatively

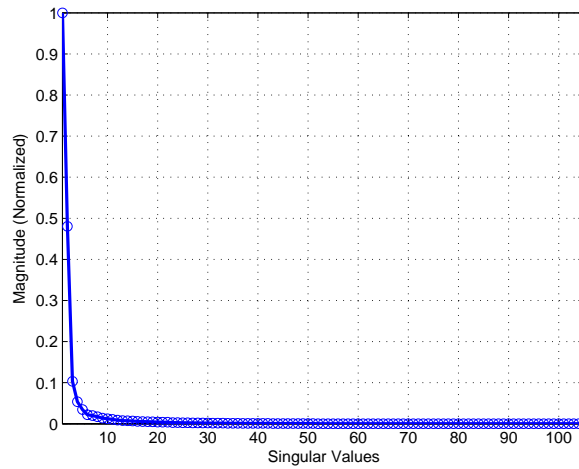


Figure 2: Normalized magnitude of singular values.

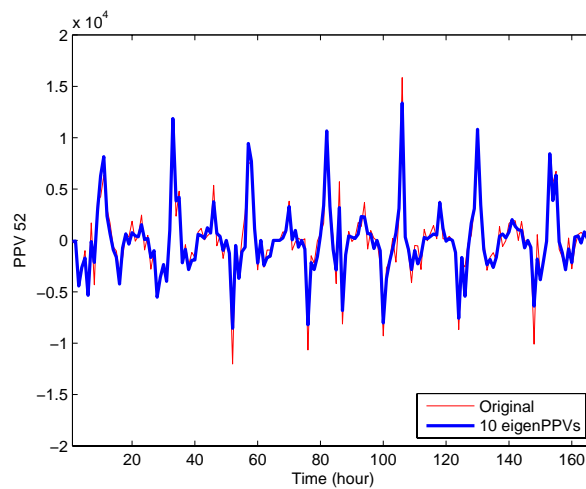


Figure 3: Reconstructing PPV 52 with 10 eigenPPVs.

greater contribution to a single PPV by eigenPPVs. The cumulative distribution function of elements is shown in Figure 5. This figure indicates that about 80% PPVs have less than 9 elements, and very few PPVs have more than 13 elements. Since PPVs consist of only a few elements, the distinction of PPVs can be inspected by their elements. Furthermore, a surprising relationship exists between the variance of a PPV and its elements. After the rows of  $\mathbf{V}$  are sorted by the variance of their corresponding PPVs, Figure 6 shows the entries whose absolute value exceed the threshold. According to the distribution of elements, two conclusions can be made. First, from the vertical direction, the elements of one PPV gather in a small region. Second, from the horizontal direction, the elements of the PPVs with larger variance are mainly significant eigenPPVs, and while the ones with smaller variance are mainly less significant eigenPPVs.

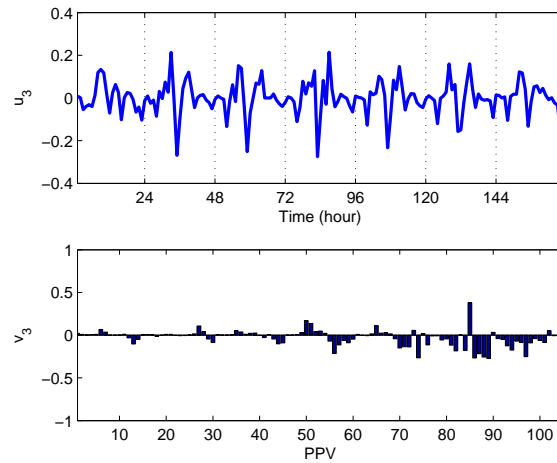
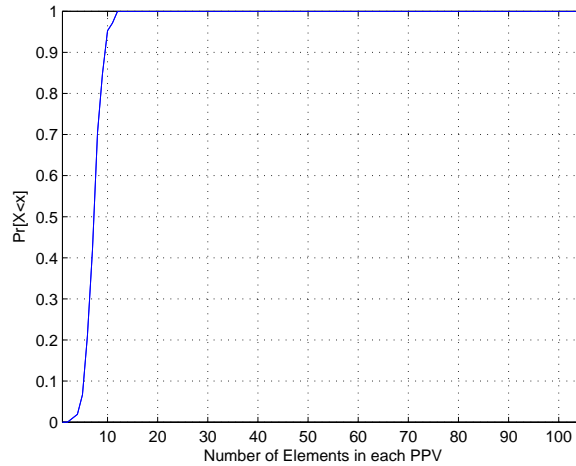
Figure 4: EigenPPV  $u_3$  and principal component  $v_3$ .

Figure 5: CDF of number of elements in each PPV.

### 3.3 Classification of EigenPPVs and Constituents of PPVs

According to their temporal features, eigenPPVs can be divided into three categories: deterministic eigenPPVs (d-eigenPPVs), spike eigenPPVs (s-eigenPPVs) and noise eigenPPVs (n-eigenPPVs), shown in Figure 7. One random eigenPPV is selected as an example of each category.

The first eigenPPV of Figure 7 shows a predictable periodic trend, reflecting the diurnal regular human activities. Due to the relative predictability, eigenPPVs of this category are called deterministic eigenPPVs. Thus, the quantitative criterion to distinguish this category of eigenPPVs is to check if there is a dominated peak in the spectrum at twenty-four hours. The second eigenPPV of Figure 7 exhibits certain strong and short-lived peaks, which indicates the occasional population migration or immigration bursts, so eigenPPVs of this category are termed as spike eigenPPVs. Since the spike description is qualitative and not rigorous, four times standard deviations criterion is employed instead: whether there is a point whose distance from the mean exceeds four times standard deviations. The last eigenPPV of Figure 7 appears to be Gaussian noise, so they are named noise eigenPPVs, capturing the random fluctuation.

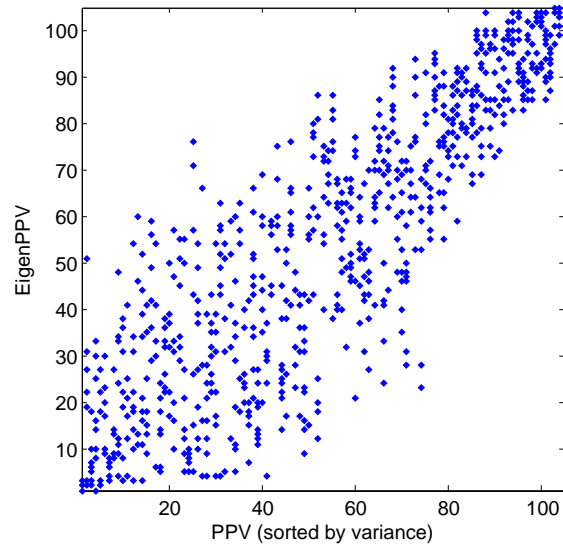


Figure 6: Elements distribution of each PPV.

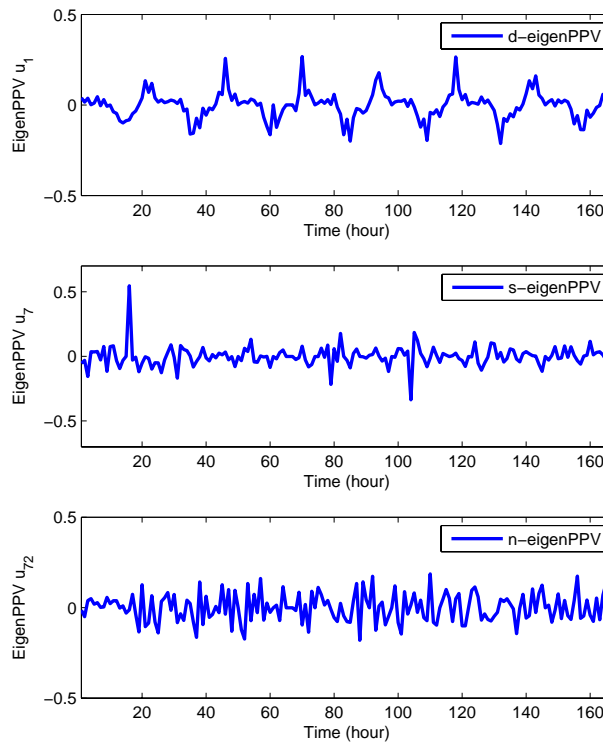


Figure 7: Examples of three categories of eigenPPVs.

The criterion of this category is to verify whether its marginal distribution is close to be Gaussian.

The category of each eigenPPV can be determined according to these three criteria above. Most of eigenPPVs fall into only one category, and only five eigenPPVs, which belong to more than one

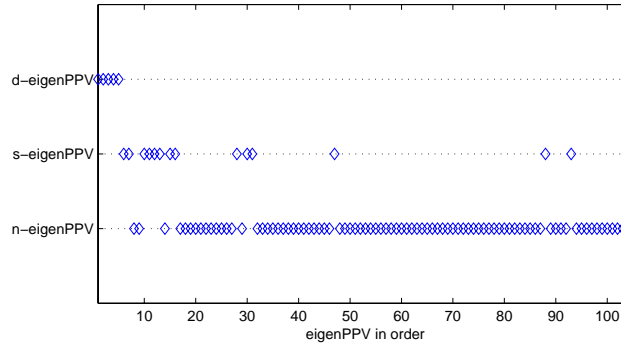


Figure 8: Categories of eigenPPVs.

category, are all insignificant. The results are showed in Figure 8. It can be seen that the five most significant eigenPPVs belong to d-eigenPPVs, most of the next ten eigenPPVs are s-eigenPPVs, and the rest less significant eigenPPVs are almost n-eigenPPVs. This association implies that periodic trends play the most critical role in urban dynamics, short-lived spikes are secondary, and noise is of the least importance.

Since each PPV can be decomposed into a weighted sum of eigenPPVs, if we add the eigenPPVs of three categories respectively, each PPV can be also decomposed into three constitutions: deterministic constitution (d-constitution), spike constitution (s-constitution), and noise constitution (n-constitution). Each constitution captures a different temporal feature of a PPV as the name implies. Figure9 shows an example, including PPV 70 and its three constitutions.

Based on this form of decomposition, an insight into the structure of PPVs can be provided by how the three constitutions vary from one PPV to another, as shown in Figure 10. (The curves are smoothed by using a moving average filter with a window size of 4.) In this figure, PPVs are sorted by variance and the fractions of the total energy contributed by three constitutions are calculated for each PPV. It indicates that there is also a relation between the variance of one PPV and its dominated constitution. The PPVs with larger variance are dominated by d-constitution. The fraction of total energy contributed by d-constitution decreases as the variance declines. The right part of the figure shows that PPVs with smaller variance are almost dominated by n-constitution. S-constitution contributes more or less equally to all the PPVs.

## 4 Applications

As stated in the previous section, the most significant eigenPPVs, which dominate the structure of the ensemble of the PPVs, belong to d-eigenPPVs. Meanwhile, if two measurement matrices of the same size only differ in the order of columns, the principal components of these two matrices are exactly the same. Thus, it indicates the temporal stability of principal components. These results about d-eigenPPVs and principal components will be quite useful in forecasting PPVs and anomaly detection. Forecasting about aggregate human mobility will no doubt benefit network planning, location management and resource management in cellular mobile networks. Meanwhile, anomaly detection can enhance temporary capacity enhancement.



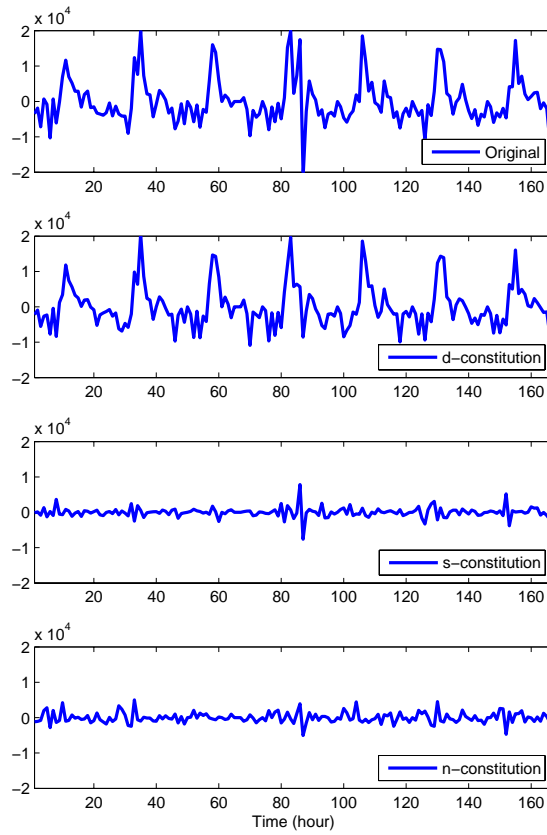


Figure 9: Decomposition of PPV 70 into three constitutions.

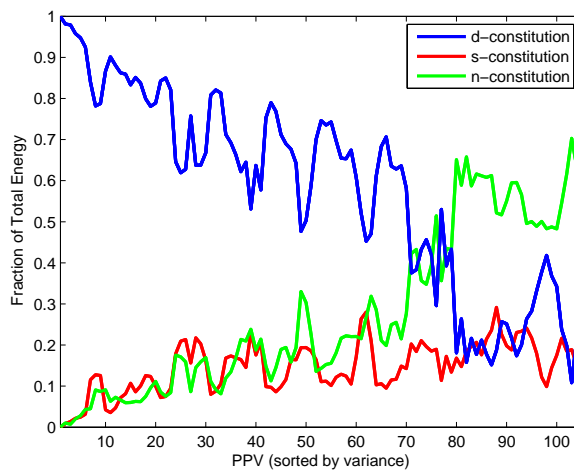


Figure 10: Fraction of total energy contributed by three constitutions of each PPV.

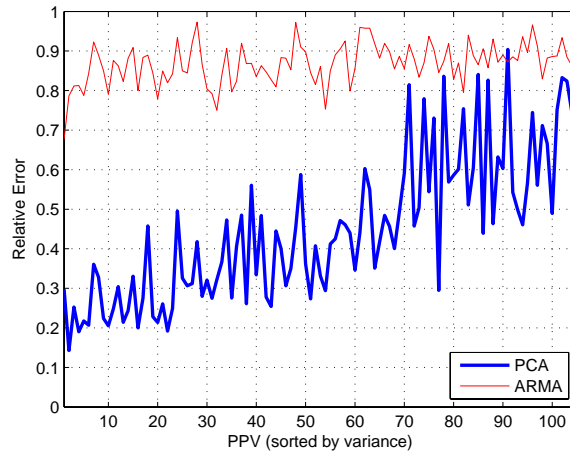


Figure 11: Performance of one-step prediction.

#### 4.1 Forecasting PPVs

A common approach to forecasting, in time series analysis, is to isolate the predictable trends based on wavelets [11]. Our method, termed as PCA model, is distinctive, and utilizes d-eigenPPVs and their corresponding principal components. Due to the temporal stability of principal components, forecasting models can be built for d-eigenPPVs, such as ARMA, based on their predictable periodic trends. Then we substitute the forecasted values of d-eigenPPVs into  $\bar{\mathbf{U}}_d$  of the following formula:

$$\bar{\mathbf{X}} = \bar{\mathbf{U}}_d \Sigma_d \mathbf{V}_d^T \quad (5)$$

where  $\bar{\mathbf{X}}$  denotes the forecasted values of all the PPVs.  $\Sigma_d$  and  $\mathbf{V}_d^T$  only retain the relevant parts of d-eigenPPVs. The forecasting range could be one moment or a certain period of time. It is worth noting that the advantage of this approach is that the forecasting can be done simultaneously for all the pixel population variations.

The performance of one-step forecast of PPVs by both ARMA model and PCA model, lasting for one week, is shown in Figure 11. The relative error of the predicted PPV  $\hat{\mathbf{a}}$  compared to original PPV  $\mathbf{a}$  is defined as:

$$RE = \frac{\|\mathbf{a} - \hat{\mathbf{a}}\|_2}{\|\mathbf{a}\|_2}$$

From the figure, it can be seen that the performance of prediction by PCA model is better than ARMA model for most PPVs. Moreover, the prediction of PPV with larger variance is relatively precise, whose fraction of total energy contributed by deterministic constitution is large.

#### 4.2 Anomaly Detection

Anomalies is usually defined as significant deviation from the general trends. So as to identify anomalies, the trends of PPVs, i.e. their d-constitutions, can be isolated by utilizing d-eigenPPVs and their corresponding principal components. Then the existence of any outlier is checked on the detrended time series based on a threshold, such as four times standard deviations. These two steps are illustrated in Figure 12.

Considering the demand of realtime detection, the notion of pseudo-eigenPPV is introduced to avoid applying PCA so often. Instead, the latest principal components are utilized to determine the pseudo-eigenPPVs based on the temporal stability of principal components. If  $\mathbf{X}$  is the new measurement matrix

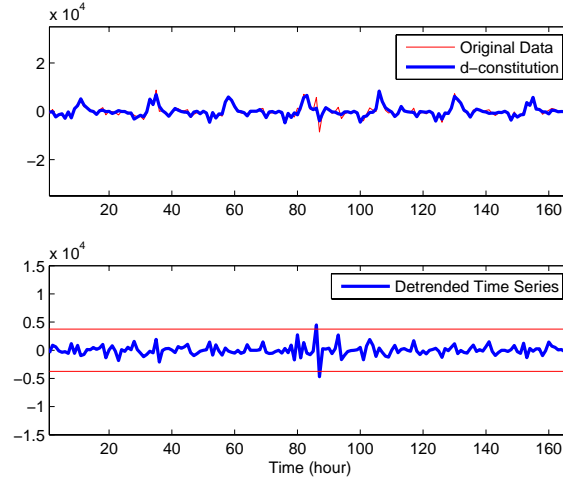


Figure 12: Example of anomaly detection in PPV 72.

and  $\{\bar{\mathbf{v}}_i\}_{i=1}^r$  are the latest principal components, the pseudo-eigenPPVs (scaled by singular value) are  $\{\mathbf{X}\bar{\mathbf{v}}_i\}_{i=1}^r$ . The trend can be determined by the most  $t$  significant pseudo-eigenPPVs as:

$$\hat{\mathbf{X}} = \sum_{i=1}^t \mathbf{X}\bar{\mathbf{v}}_i\bar{\mathbf{v}}_i^T \quad (6)$$

Then the detrended time series, columns of  $\mathbf{X} - \hat{\mathbf{X}}$ , will be tested by the four times standard deviations criterion.

## 5 Conclusion and Future Work

In this paper, PCA is utilized to analyze the space-time structure of aggregate human mobility in urban space. Based on the results of analysis, a low intrinsic dimensionality is revealed, which indicates that the ensemble of PPVs can be accurately approximated by a small set of eigenPPVs, even though there are hundreds of PPVs. Each PPV can be decomposed into a weighted sum of eigenPPVs. Furthermore, the variance of one PPV is related to its elements, an notion representing the components with relatively greater contribution by eigenPPVs. According to the temporal features, there appear to be three categories of eigenPPVs: d-eigenPPVs, s-eigenPPVs and n-eigenPPVs, and the most significant significant eigenPPVs almost belong to d-eigenPPVs, which implies that the predictable periodic trends dominate the structure of the ensemble of PPVs.. According to this classification, each PPV is decomposed into three constitutions: d-constitution, s-constitutions and n-constitutions, which represent deterministic trends, short-lived spikes and noise, respectively. The contributions of the three constitutions vary from one PPV to another, and also have a relationship with its variance. D-eigenPPVs and its domination in the structure play a critical role in the applications of forecasting PPVs and anomaly detection.

There are two directions for future work. One direction is the specific applications in engineering. Although the original data is collected from cellular wireless networks, accurate modeling of aggregate human mobility will definitely benefit mobility management and resource management in the design of many other wireless networks. The other one is the mathematical tools for analyzing. PCA is a linear dimension reduction technique which limits the functionality of its own, though it performs well here

in exploring the structure of urban dynamics. Other non-linear dimension reduction techniques may be utilized to reveal some other valuable insights.

## Acknowledgment

This work is supported in part by the National Basic Research Program of China (973 Program) under grants 2007CB307100 and 2007CB307105.

## References

- [1] R. Ahas and Ü. Mark. Location based services—new challenges for planning and public administration? *Futures*, 37(6):547–561, 2005.
- [2] C. Bettstetter. Mobility modeling in wireless networks: Categorization, smooth movement, and border effects. *ACM Mobile Computer and Comm. Rev.*, 5(3):17–29, 2001.
- [3] F. Calabrese and C. Ratti. Real time rome. *Networks and Communication Studies*, 20:247–258, 2006.
- [4] N. Eagle and A. Pentland. Reality mining: Sensing complex social systems. *Personal and Ubiquitous Computing*, 10(4):255–268, 2006.
- [5] G. H. Golub and C. Reinsch. Singular value decomposition and least squares solutions. *Numerische Mathematik*, 14(5):403–420, 1970.
- [6] M.C. González, C.A. Hidalgo, and A.L. Barabási. Understanding individual human mobility patterns. *Nature*, 453(7196):779–782, 2008.
- [7] H. Hotelling. Analysis of a complex of statistical variables into principal components. *J. Educ. Psy.*, pages 417–441, 1933.
- [8] A. Lakhina, Konstantina Papagiannaki, Mark Crovella, Christophe Diot, Eric D. Kolaczyk, and Nina Taft. Structural analysis of network traffic flows. *ACM SIGMETRICS Performance Evaluation Review*, 32(1):61–72, 2004.
- [9] D. Lam, D.C. Cox, and J. Widom. Teletraffic modeling for personal communications services. *IEEE communications magazine*, 35(2):79–87, 1997.
- [10] E. O’Neill, V. Kostakos, T. Kindberg, A. Schiek, A. Penn, D. Fraser, and T. Jones. Instrumenting the city: Developing methods for observing and understanding the digital cityscape. *UbiComp 2006: Ubiquitous Computing*, pages 315–332, 2006.
- [11] K. Papagiannaki, N. Taft, Z.L. Zhang, and C. Diot. Long-term forecasting of internet backbone traffic: Observations and initial models. In *IEEE INFOCOM, San Francisco*, April 2003.
- [12] C. Ratti, S. Williams, D. Frenchman, and RM Pulselli. Mobile Landscapes: using location data from cell phones for urban analysis. *ENVIRONMENT AND PLANNING B PLANNING AND DESIGN*, 33(5):727, 2006.
- [13] J. Reades, F. Calabrese, and C. Ratti. Eigenplaces: analysing cities using the space-time structure of the mobile phone network. *Environment and Planning B: Planning and Design*, 36:824–836, 2009.
- [14] J. Reades, F. Calabrese, A. Sevtsuk, and C. Ratti. Cellular census: explorations in urban data collection. *Pervasive Computing*, 6(3):30–38, 2007.
- [15] J. Sun, Y. Wang, H. Si, X. Mao, J. Yuan, and X. Shan. A PCA-based approach for exploring space-time structure of urban mobility dynamics. In *Proceedings of the 6th International Wireless Communications and Mobile Computing Conference Workshop on Mobility Modeling and Performance Evaluation (MoMoPE)*, pages 859–863, 2010.
- [16] R. Thomas, H. Gilbert, and G. Mazziotto. Influence of the moving of the mobile stations on the performance of a radio mobile cellular network. In *Proc. 3rd Nordic Seminar on Digital Land Mobile Radio Communications*, 1988.
- [17] Rongrong Xu, Wei Feng, and Feng Zhou. The exploration of mobile network-based grid system of presenting population density distribution. *Science and Technology Management Research*, 7:334–335, 2008.



**Jingbo Sun** is a Ph.D. candidate in the Department of Electronic Engineering at Tsinghua University. He received his B.S. degree from the School of Electronics and Information Engineering at Harbin Institute of Technology in 2006. His research interests include wireless networks and mobility management.



**Yue Wang** received his Ph.D. degree from the Electronic Engineering Department of Tsinghua University in 2005. He is now an assistant professor at Tsinghua University. His research interests include computer networks and data fusion.



**Hongbo Si** received his B.S. and M.S. degrees in Tsinghua University in 2007 and 2010 respectively. He is a Ph.D. student in the University of Texas at Austin at present. His research interests include wireless networks and information theory.



**Jian Yuan** received his Ph.D. degree in electrical engineering from the University of Electronic Science and Technology of China, in 1998. He is currently an associate professor in the Department of Electronic Engineering at Tsinghua University, Beijing, China. His core interest is complex dynamics of networked systems, and dependability of mobile networks.



**Xiuming Shan** received his B.S. degree from the Electronic Engineering Department of Tsinghua University in 1970. He is the head and chair professor of Institute of High-speed Signal Processing and Network Transmission, Electronic Engineering Department, Tsinghua University. His research includes radar signal processing, computer networks, and complex systems.